Hindawi
Wireless Communications and Mobile Computing
Volume 2022, Article ID 4147373, 14 pages
https://doi.org/10.1155/2022/4147373

Research Article

The Optimal Packets Scheduling for Buffer-Aid Energy Harvesting RSUs in Cooperative Vehicle Infrastructure System

Ying Shi,[1,2] Chi Feng,[1] Tong Wang,[1] Qingjiang Yang,[2] and Yiping Chen[2]

[1]*College of Information and Communication Engineering, Harbin Engineering University, Harbin 150001, China*
[2]*School of Electric and Information Engineering, Heilongjiang University of Science and Technology, Harbin 150022, China*

Correspondence should be addressed to Yiping Chen; sy_hit2004@163.com

Received 10 February 2022; Accepted 1 April 2022; Published 26 April 2022

Academic Editor: Han Liu

In this paper, we investigate the optimal packet scheduling for RSU-to-vehicle downlink communication in Cooperative Vehicle Infrastructure System (CVIS). The RSU is powered by a capacity-limited battery storing harvested energy with reliable energy source as backup, which meets requirement of renewable energy and ensures sustainability of communication system. We aim to find the optimal packet scheduling policy that minimizes the data queuing delay under a given the reliable power constraint and downlink availability rate. According to probabilistic scheduling policy, we adopt data buffer queue and harvesting energy queue as the state-space, and determine the transition action by the joint state of packet arrivals and channel state to establish a two-dimensional Markov chain. Based on this, the optimization problem is formulated. By solving the problem and analysing its solution, we derive the optimal transmission parameters and the optimal scheduling policy which turns out to be threshold-based. Simulations are demonstrated to verify the accuracy of the theoretical derivation results.

1. Introduction

1.1. Motivations. Internet of Vehicles (IoV) is the application of Internet of Things (IoT) in urban traffic, which promotes the development of urban intelligent transportation system (ITS). At present, the Cooperative Vehicle Infrastructure System (CVIS) has become one of the most promising and fastest growing research in ITS. In CVIS, accurate and timely information interaction between vehicles and infrastructure can contribute to solve intelligent information management and decision-making problems, such as traffic congestion and road safety problems [1, 2]. Data transmission is completed in the way of "store-carry-forward" through passing vehicles within roadside units (RSUs) coverage. Therefore, the RSUs are not only important network access equipment with providing high-speed message forwarding services for vehicles over high bandwidth links, but also gateway nodes of the surrounding environmental monitoring sensor network, which undertakes the function of transmitting monitoring data to roadside units connected with the Internet [3, 4]. Nevertheless, the high-speed and high bandwidth forwarding services require high power consumption [5]. In addition, the RSUs are powered by the electrical grid instead of no-renewable energy, which costs too much, and increased usage of such energy resources will lead to increase carbon dioxide emission. Thereby, renewable and harvested energy resources, such as solar energy, wind energy and RF energy, are generally considered as substitute for conventional grid power [6].

However, harvested energy arrives randomly and sporadically due to environmental influence, such as weather and geographic position, etc. To avoid excessive energy and save for future use, battery is used to save the collected energy, but the capacity is usually limited and inconsistent availability [7]. It is possible that RSUs powered by harvested energy alone may not guarantee the quality of service. Thus, the use of conventional grid power cannot be eliminated. When renewable energy sources are not available, using grid energy as a substitute power supply can minimize grid consumption, which will help in reducing energy cost and harmful emission. Hence, there is a hybrid energy supplies formed by harvesting energy and reliable power (for example, grid power) to ensure quality of service and the communication sustainability [8, 9]. In fact, the RSU is mainly powered by harvested energy and the grid is used as a backup.

In the above scenario, guaranteeing data timeliness under the constraint of reliable power consumption is a most important metrics when dealing with the packet scheduling optimization of each RSU. Nevertheless, this is not easy. First, in order to achieve efficient data dissemination, there is usually the cooperation of hybrid infrastructure-to-vehicle (I2V) and vehicle-to-vehicle (V2V) communication in CVIS, which makes the data conflicts in the RSU coverage area, causing the interference in the establishment of data communication links, and directly affecting the data transmission timeliness [10, 11]. Second, the RSU is encouraged to use the free and renewable energy whenever available, but the waiting time could be undesirably long if it only relies on the harvested energy. Third, even if a reliable energy is available when renewable energy is unavailable, power consumption limit makes it impossible to use indefinitely, and it will increase the waiting time. To address the above issues, it is necessary to jointly research data transmission delay-minimal and power-constrained trade-off problem to ensure the RSU-to-vehicle downlink data communication timeliness with using grid power as little as possible.

1.2. Related Works. In recent years, the use of energy harvesting RSUs in vehicular environment has gradually received the attention in the research literature. In [12], the design of a solar energy harvesting circuit RSUs is presented, and the usability of energy harvesting systems in vehicular networks is investigated in [13]. In [14], the authors use a smart scheduling to reduce RSU energy costs in green vehicular roadside infrastructure, and the authors of [8] assumed that RSUs are powered by both grid source and renewable energy, and proposed an efficient sleep scheduling method to an overall decrease of energy cost. Several works have been carried out recently for optimal scheduling in RSU-to-vehicle communication. The main contribution of [15] is to investigate the problem of scheduling the downlink communication from renewable energy-powered RSUs toward vehicles, with the objective of maximizing the number of served vehicles. For the purpose of optimizing the RSU's downlink traffic scheduling, a protocol for energy-efficient adaptive scheduling using reinforcement learning is proposed, focusing on guaranteeing the operation of the vehicular network [16]. Regarding to energy consumption and time delay minimal in the CVIS, packet scheduling optimization strategy for energy-delay trade-off in self-powered RSUs is proposed [17, 18]. And a rudimentary online scheduling algorithm for estimating the energy consumption, average packet delay and required battery capacity is proposed [19].

In the process of RSU-to-vehicle communication, it involves data arrival, queuing behaviour, power allocation and data transmission in RSUs, corresponding to the network layer, the data link layer and physical layer, respectively. The cross-layer has been proved as one of the most efficient solutions for wireless communications involving multiple layers [20–23]. The cross-layer method was firstly studied in [20], where the scheduling policy is studied for transmission under a time-varying channel with delay constraint. In [21], the sensing-throughput trade-off crosses physical layer and MAC layer in multi-channel cognitive radio networks. In [22], the authors achieved energy efficient and delay trade-off using cross-layer stochastic optimization approach. In addition, it is well applied to green vehicular networks [23].

1.3. Contributions. In this work, we address an optimal resource scheduling for the RSU powered by both grid-powered and energy harvesting in RSU-to-vehicle downlink communication. The objective is to minimize the packet queuing delay given the available power constraint with considering the connectivity probability between RSU and vehicle. To analyse the proposed scheme, we adopt the cross-layer framework by combining the data packet arrival in the network layer, queuing state in the MAC layer, and transmission over the wireless channel as well as the energy harvesting behaviour in the physical layer. Then, we formulate a probability scheduling, considering the joint state of random energy arrivals, random data packet arrivals and time-varying channel states. Based on the scheduling, we draw up a two-dimensional Markov chain by using both data queue and harvested energy queue as state variables, and formulate an optimal scheduling problem to describe the delay minimal and reliable power consumption trade-off. With the solution to the optimization problem, the optimal scheduling policy can be revealed as a threshold-based policy. At the end, our theoretical analysis is verified by simulations.

2. System Model

We consider a packet transmission scenario between RSUs relayed by vehicle is shown in Figure 1. For sake of reducing environmental pollution, the RSU is powered by two sources of energy namely, a fixed power line using the conventional grid energy and Photo Voltaic cells to utilize the solar energy, but grid power is only used to ensure that the RSU is always operational when necessary [8]. The collected data (such as surrounding traffic, monitoring information) is stored in the data buffer of RSU, waiting to be sent to another RSU with data aggregation centre in form of packet queuing through mobile vehicles transmission. To improve the connectivity probability of vehicular communication, vehicle may complete the whole data transmission through a wireless multi-hop path with V2V communication [24]. However, in this paper, we only focus on the downlink communication from RSU-to-vehicle. Considering the discrete time-slotted system, in a certain time slot, if RSU does not establish a downlink communication link with passing vehicles, the data packet will wait in the buffer. However, if the downlink link is available, RSU determines whether to send packets to passing vehicles and the corresponding power consumption according to the packet scheduling strategy.

In Figure 2, we formulate a cross-layer system model. At the RSU, the data packets (such as monitoring data)

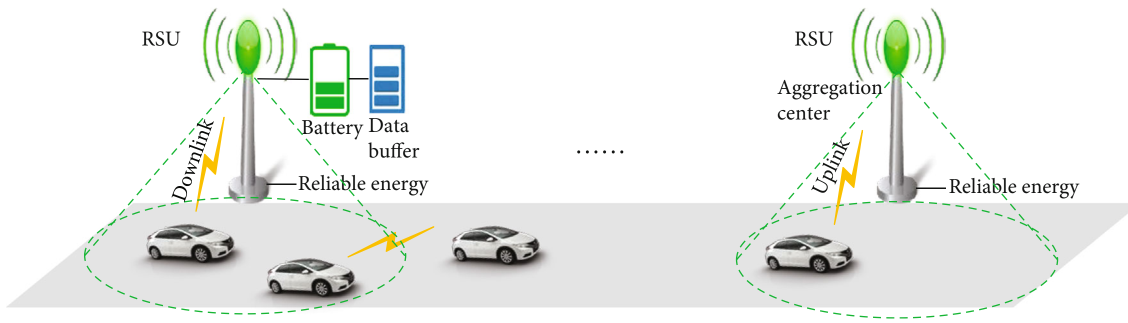

Figure 1: Schematic diagram of RSU-to-vehicle scene.

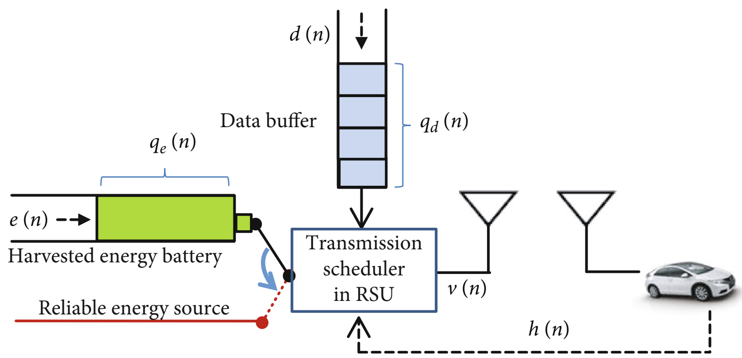

Figure 2: A cross-layer system model.

generated by the upper layers arrive at the MAC layer and are stored at a data buffer. A battery storing the free and renewable energy harvested from the environment is represented in a virtual queue. If a downlink link has been established in the slot, the RSU will combine the data buffer status, energy queue status and new packet arrival to determine whether to send data packet to the vehicle according to the packet scheduling strategy, so as to control the reliable energy consumption and queuing delay of data.

2.1. Packet Arrival Model. In discrete-time slotted system, assuming that packets are generated randomly, following the Bernoulli process, we can define that the data packets randomly arrive with rate η_d. Each data arrival contains $k_d \in \mathbb{N}^+$ packets. Let $d[n]$ denotes the number of packets arriving at the RSU at the beginning of the n-th timeslot. The mass probability function of $d[n]$ is given by

$$\begin{aligned} \Pr\{d[n]=k_d\} &= \eta_d \\ \Pr\{d[n]=0\} &= \bar{\eta}_d, \end{aligned} \quad (1)$$

where $\eta_d \in [0,1]$ and $\bar{\eta}_d = 1-\eta_d$. At the RSU, a buffer is adopted to store the packets that cannot be sent immediately, and its capacity is expressed by Q_d. Let $v_d[n]$ and $q_d[n]$ note the number of packets transmitted in the n-th slot and the queue length at the end of n-th timeslot, respectively. Thus, the update of the data packet queue can be obtained as

$$q_d[n] = \min\{q_d[n-1]+d[n], Q_d\} - v_d[n] \quad (2)$$

In Figure 2, the RSU can harvest energy from the environment. The energy storage and consumption processes of the battery can be described as a queuing system. In particular, the harvested energy packets arrive randomly following a certain distribution, and leave the queue when the scheduler spends a few energy packets for data packet transmission. There also exists an upper limit Q_e for the virtual queue corresponding to the storage capacity of the battery. This means that the battery can store at most Q_e energy packets, each of which contains a certain amount of energy. $q_e[n]$is used to measure the length of the energy queue, i.e., the remaining energy in the battery. We use $e[n]$ describe the process of energy harvesting. Suppose that a certain amount of energy is harvested each time. Accordingly, $k_e \in \mathbb{N}^+$ energy packets arrive at the battery with probability η_e. Therefore, the mass probability function of $e[n]$ is given by

$$\begin{aligned} \Pr\{e[n]=k_e\} &= \eta_e \\ \Pr\{e[n]=0\} &= \bar{\eta}_e, \end{aligned} \quad (3)$$

where $\eta_e \in [0,1]$means the energy arrival rate, and $\bar{\eta}_e = 1-\eta_e$. Let $v_e[n]$ notes number of energy packets consumed in n-th timeslot. Similarly, the update of the energy queue is characterized as

$$q_e[n] = \min\{q_e[n-1]+e[n], Q_e\} - v_e[n] \quad (4)$$

2.2. Transmission Channel Model. In Figure 1, all the data packets in the RSU will be transmitted to the vehicle through wireless channel, which is supported by dedicated short range communication (DSRC) protocol. However, in the

CVIS, the vehicle can only establish communication connection with RSU within its coverage. When the vehicle drives out the coverage of RSU, the connection will be disconnected. Therefore, there are two communication channel states of "*on*/*off*" between RSU and vehicle, which represent the working state and offline state between vehicle and RSU. Moreover, within the coverage aera of RSU, there are not only RSU-to-vehicle downlink transmission channels, but also vehicle-to-vehicle transmission channels, which may interfere with each other. It cannot be guaranteed that the downlink communication channels between RSU and vehicle are available in each time slot. So, in this paper, we use "*on*" and "*off*" to describe the channel state, which is denoted by $h[n]$ in the n-th timeslot. The mass distribution function of the state is given by

$$\begin{aligned} &\Pr\left\{h[n] = {'on'}\right\} = \alpha \\ &\Pr\left\{h[n] = {'off'}\right\} = \bar{\alpha}, \end{aligned} \tag{5}$$

where α represents the probability that the downlink channel remains working, namely "*on*," while $\bar{\alpha}$ represents the probability that the downlink channel remains offline, namely "*off*," and $\alpha + \bar{\alpha} = 1$ in n-th timeslot.

2.3. Probabilistic Scheduling Policy. For convenience of analyse, the RSU is supposed to successfully deliver one data packet with one energy packet from the energy queue or with grid power in watts when the channel state is "*on*." Usually, the scheduler prefers to use the harvested energy because it is free and renewable, which is also desirable. However, due to the uncertainty of external environment, it may have to wait a long time to harvest sufficient power for next packet transmission, which is intolerable for latency-sensitive application. In this situation, reliable power source should be adopted instead. However, if the RSU relies too much on the reliable power source, the communication cost will increase inevitably, which is inconsistent with the original intention. Thus, there exists a trade-off between the queuing delay and the transmission power drawn from the reliable energy source. In this work, the scheduler aims to find an optimal scheduling strategy to minimize the average queuing delay constrained by the grid power.

Let $\boldsymbol{v}[n] = (v_d[n], v_e[n])$ note the actions taken in the n-th slot, namely, transmitting $v_d[n]$data packets with $v_e[n]$ energy packets. The transmission channel state plays a key role, because it be possible to transmit data packets only when $h[n] = {'on'}$. Specifically, when the harvested energy is enough for one transmission, one data packet should always be transmitted to decrease the buffer occupation. Otherwise, the scheduler must decide whether to transmit with a certain grid power in current timeslot. Simultaneously, we define the joint state vector $\boldsymbol{s}[n] = (d[n], e[n], h[n])$ and the queue state vector $\boldsymbol{q}[n] = (q_d[n], q_e[n])$. Based on the packet arrival and queuing states, the scheduling policy can be described below in three cases.

Case 1. when $\boldsymbol{q}[n-1] = (i, 0), (i \geq 0)$,

$$\boldsymbol{v}[n] = \begin{cases} (1,1)\, w.p.1 & \boldsymbol{s}[n] = \left(\cdot, k_e, {'on'}\right) \\ (1,0)\, w.p.g_i & \boldsymbol{s}[n] = \left(k_d, 0, {'on'}\right) \\ (1,0)\, w.p.f_i & \boldsymbol{s}[n] = \left(0, 0, {'on'}\right) \\ (0,0) & otherwise \end{cases} \tag{6}$$

where "*w.p.*" is short for "with probability of" and the symbol "·" in the expression of $\boldsymbol{s}[n]$ means no matter how many packets (data packet or energy packet) arrive in this slot. Let $\{g_i\} \in [0,1]$ and $\{f_i\} \in [0,1]$ be the probabilities of packet transmission with or without packet arrivals in this time slot, respectively. Accordingly, it is also possible for the RSU to remain silent with probabilities $1 - g_i$ and $1 - f_i$, respectively. In this case, there are data packets waiting in the data buffer but no renewable energy packet can be used for transmitting in RSU. Taking the first term in (6) for example, when the channel is "*on*," regardless of the data packet arrival state, one packet will be delivered $v_d[n]$ at the cost of one energy packet $v_e[n]$ if k_e energy packets being harvested. As for the second term, there is no energy packet newly harvested. Thus, the scheduler decides to transmit one data packet $v_d[n] = 1$ with probability $g_i (i \geq 0)$ using paid reliable power $v_e[n] = 1$, otherwise, remain silent $v_d[n] = 0$ with probability $1 - g_i$. Similarly, when no data packets newly arrive, the RSU would transmit one packet using the paid power with probability $f_i (i > 0)$ or remain silent $v_d[n] = 0$ with probability $1 - f_i$, respectively. Whether the packets are reached or not, only if the channel state is offline, then $\boldsymbol{v}[n] = (0, 0)$.

Case 2. when $\boldsymbol{q}[n-1] = (i, j), (i, j > 0)$,

$$\boldsymbol{v}[n] = \begin{cases} (1,1)\, w.p.1 & \boldsymbol{s}[n] = \left(\cdot, \cdot, {'on'}\right) \\ (0,0)\, w.p.1 & \boldsymbol{s}[n] = \left(\cdot, \cdot, {'off'}\right) \end{cases} \tag{7}$$

In this case, both data buffer and energy queue are not empty. Then, no matter whether the new data and harvested energy packets arrive in n-th slot, a data packet will be delivered with an energy packet if the downlink channel is available.

Case 3. when $\boldsymbol{q}[n-1] = (0, j), (j > 0)$,

$$\boldsymbol{v}[n] = \begin{cases} (1,1)\, w.p.1 & \boldsymbol{s}[n] = \left(k_d, \cdot, {'on'}\right) \\ (0,0)\, w.p.1 & \boldsymbol{s}[n] = \left(0, \cdot, {'on'}\right) \\ (0,0)\, w.p.1 & \boldsymbol{s}[n] = \left(\cdot, \cdot, {'off'}\right) \end{cases} \tag{8}$$

In this case, there are enough harvested energy storing at the battery but the data queue is zero. Then, one energy

Table 1: The one-step transition probabilities $\Pr\{\boldsymbol{q}[n]|\boldsymbol{q}[n-1]\}$.

$\boldsymbol{q}[n\text{-}1]$	$\boldsymbol{q}[n]$	$\Pr\{\boldsymbol{q}[n]\|\boldsymbol{q}[n-1]\}$	$\boldsymbol{q}[n\text{-}1]$	$\boldsymbol{q}[n]$	$\Pr\{\boldsymbol{q}[n]\|\boldsymbol{q}[n-1]\}$
(i, j)	$(i\text{-}1, (j+k_e)\vee Q_e\text{-}1)$	$\rho_0\alpha$	(i, j)	$(i, j+k_e)$	$\rho_0\bar{\alpha}$
(i, j)	$(i\text{-}1, j\text{-}1)$	$\rho_1\alpha$	(i, j)	(i, j)	$\rho_1\bar{\alpha}$
(i, j)	$(i+k_d\text{ -}1, j\text{-}1)$	$\rho_2\alpha$	(i, j)	$(i+k_d, j)$	$\rho_2\bar{\alpha}$
(i, j)	$(i+k_d\text{ -}1, (j+k_e)\vee Q_e\text{-}1)$	$\rho_3\alpha$	(i, j)	$(i+k_d, j+k_e)$	$\rho_3\bar{\alpha}$
$(i, 0)$	$(i+k_d\text{ -}1, 0)$	$\rho_2\alpha g_i$	$(i, 0)$	$(i+k_d, 0)$	$\rho_2\alpha(1-g_i)+\rho_2\bar{\alpha}$
$(i, 0)$	$(i\text{-}1, 0)$	$\rho_1\alpha f_i$	$(i, 0)$	$(i, 0)$	$\rho_1\alpha(1-f_i)+\rho_1\bar{\alpha}$
$(0, j)$	$(0, (j+k_e)\vee Q_e)$	ρ_0	$(0, j)$	$(0, j)$	ρ_1
(i, Q_e)	$(i\text{-}1, Q_e\text{-}1)$	$\bar{\eta}_d\alpha$	(i, Q_e)	$(i+k_d\text{-}1, Q_e\text{-}1)$	$\eta_d\alpha$
(i, Q_e)	(i, Q_e)	$\bar{\eta}_d\bar{\alpha}$	(i, Q_e)	$(i+k_d, Q_e)$	$\eta_d\bar{\alpha}$
$(i, Q_e\text{-}1)$	(i, Q_e)	$\rho_0\bar{\alpha}$	$(0, Q_e)$	$(0, Q_e)$	$\bar{\eta}_d$
$(0, Q_e\text{-}1)$	$(0, Q_e)$	ρ_0	$(0, 0)$	$(0, 0)$	ρ_1

packet is spent for delivering one data packet newly arriving. And if no packets arrive at n-th slot, or the channel is offline, there is no energy consumption.

2.4. Markov Chain Model. Based on the probabilistic scheduling policy, we know that the transmission decision is made only in each time slot based on the queuing state $\boldsymbol{q}[n-1]$ and the joint states$\boldsymbol{s}[n]$, Hence, the queuing system can be characterized by a two-dimensional Markov chain with $\boldsymbol{q}[n]$ being the state variables $\{(i,j)|i=0,\cdots,Q_d\,;j=0,\cdots,Q_e\}$. For simplicity, we firstly define the following four joint probability parameters about packets arrival, shown as

$$\begin{cases}\rho_0=\Pr\{d[n]=0,e[n]=k_e\}=\bar{\eta}_d\eta_e\\ \rho_1=\Pr\{d[n]=0,e[n]=0\}=\bar{\eta}_d\bar{\eta}_e\\ \rho_2=\Pr\{d[n]=k_d,e[n]=0\}=\eta_d\bar{\eta}_e\\ \rho_3=\Pr\{d[n]=k_d,e[n]=k_e\}=\eta_d\eta_e\end{cases} \tag{9}$$

According to the scheduling scheme defined by the formulas (6)-(8), we focus on deriving the one-step state transition probability $\Pr\{\boldsymbol{q}[n]|\boldsymbol{q}[n-1]\}$ between states, which are listed in Table 1 in detail. In Table 1, the $(j+k_e)\vee Q_e$ denotes $\min\{(j+k_e),Q_e\}$, and the state transition probabilities locating below dashed line are the special case what i=0 or $j=\{0,Q_e-1,Q_e\}$. Except for the special states, the rest state transition probabilities $\Pr\{\boldsymbol{q}[n]|(i,j)\}$ are exhibited above the dashed line. In particular, the case $j=Q_e$ requires special processing, because the battery is full and the newly harvested energy must be discarded. Besides, the case $j=Q_e-1$ also discard the remaining packets when the packet number of newly harvested energy exceeds 1.

Based on Table 1, we construct a 2D Markov chain model shown in Figure 3, where solid lines present the fixed state transitions while all dotted lines indicate state transitions that vary with different k_d and k_e. To check the transition probability given in Table 1, assume $k_d=k_e=2$in Figure 3. Let $m,n\in\{0,1,2,3\}$, we modify the definition of variable α as, $\alpha_m=\rho_m\alpha$, $\bar{\alpha}_m=\rho_m\bar{\alpha}$ in Figure 3. Moreover, the scheduler makes a decision of transmission with a probability only under the situation that there are no harvested energy packets can be used, that is the state transition between states (i,0). We define four variables $\lambda_{1,i}=\rho_2\alpha g_i$, $\lambda'_{1,i}=\rho_2\alpha(1-g_i)+\rho_2\bar{\alpha}$, $\mu_{1,i}=\rho_1\alpha f_i$, $\mu'_{1,i}=\rho_1\alpha(1-f_i)+\rho_1\bar{\alpha}$ on the first column in Figure 3.

For ease of discussion, we give the simplified Markov chain which is shown in Figure 4, where the transition probabilities are obtained from the substitution of $k_d=1$, $k_e=1$ in Figure 3. For example, the transition from (i,j) to $(i+k_d-1,j)$ in Figure 3 becomes that from (i,j) to (i,j) in Figure 4, for $i,j>0$. For this state transition, one is that both data and energy packet arrive and the transmission link is available so that a data is delivered with the corresponding probability of α_3, the other is neither data nor energy packet arrives and the transmission link is unavailable, so that no backlogged data packet is transmitted with the corresponding probability $\bar{\alpha}_1$. Therefore, a new notation is needed for the transition from (i,j) to (i,j), which $\bar{\alpha}_1+\alpha_3$, namely, α', for $i,j>0$. The transition between these states in Figure 4 can easily derived based on the dynamic change of the data buffer queue and the virtual energy queue as given in (2) and (4).

Denote by $\boldsymbol{\pi}_i$, $\boldsymbol{\pi}_j$ and $\pi_{(i,j)}$ the steady-state probabilities of the data queue state, the energy queue state and the joint queue state, respectively. The relationship between the steady-state probabilities of the 2D Markov chain can be represented in the following theorem.

Theorem 1. *Define $\tilde{\mu}_{1,i}=\rho_1\alpha f_i+\alpha_0$, then the local balance equations of the Markov chain is obtained as*

$$\begin{aligned}&\tilde{\mu}_{1,i}\pi_{(i,0)}+\alpha_0\sum_{j=1}^{Q_e}\pi_{(i,j)}+\alpha_1\sum_{j=1}^{Q_e}\pi_{(i,j)}\\ &\quad=\pi_{(i-1,0)}\lambda'_{1,i-1}+\bar{\alpha}_2\sum_{j=1}^{Q_e}\pi_{(i-1,j)}+\bar{\alpha}_3\sum_{j=0}^{Q_e}\pi_{(i-1,j)}\end{aligned} \tag{10}$$

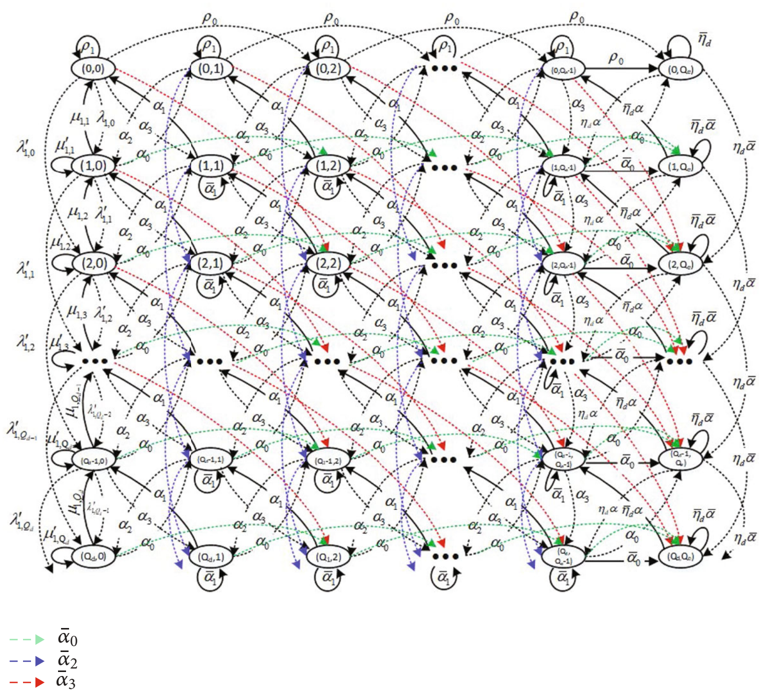

FIGURE 3: The two-dimensional Markov chain model.

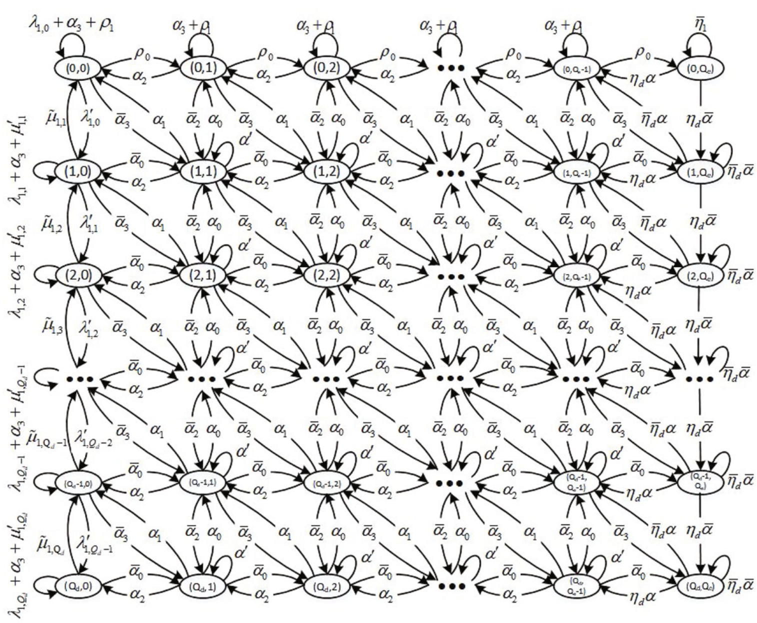

FIGURE 4: The two-dimensional Markov chain model.

The expression of steady-state probabilities of the data queue $\boldsymbol{\pi}_i$ *can be derived as*

$$\boldsymbol{\pi}_i = \sum_{j=0}^{Q_e} \pi_{(i,j)} \tag{11}$$

With the definition of $\boldsymbol{\pi}_i$, $\alpha_0 + \alpha_1 = \bar{\eta}_d \alpha$, and $\bar{\alpha}_2 + \bar{\alpha}_3 = \eta_d \bar{\alpha}$, we can then reformulate (10), as following

$$\bar{\eta}_d \alpha \boldsymbol{\pi}_i - \eta_d \bar{\alpha} \boldsymbol{\pi}_{i-1} = \left(\lambda'_{1,i-1} - \bar{\alpha}_2\right)\pi_{(i-1,0)} + \left(\bar{\eta}_d \alpha - \tilde{\mu}_{1,i}\right)\pi_{(i,0)} \tag{12}$$

Let $\boldsymbol{\Lambda}$ denote the transition probability matrix, we know that the steady-state probability $\pi_{(i,j)}$should meet constraint $\boldsymbol{\Lambda\pi} = \boldsymbol{\pi}$, where vector $\boldsymbol{\pi}$ is defined as $[\pi_{(0,0)}, \pi_{(0,1)} \cdots \pi_{(0,Q_e)}, \pi_{(1,0)}, \pi_{(1,1)} \cdots \pi_{(1,Q_e)}, \cdots, \pi_{(Q_d,0)}, \pi_{(Q_d,1)} \cdots \pi_{(Q_d,Q_e)}]$. Also, $\pi_{(i,j)}$

should meet the normalization constraint, namely, $\sum_{i=0}^{Q_d}\sum_{j=0}^{Q_e}\pi_{(i,j)} = 1$.

3. Establishment of Optimization Problem

At the above section, we have illustrated the fundamental trade-off between queuing delay and transmission power paid at cost in the RSU. It is of great significance to derive the average queuing delay and the power consumption mathematically. In this section, we will discuss the delay and power metrics based on the properties of two-dimensional Markov chain model in Figure 4.

3.1. The Delay and Power Metrics. Since the average queuing delay is associated with the occupancy rate of the data queue, combined with the steady-state probabilities of the data queue, the average occupancy rate of the data queue can be obtained as $\sum_{i=1}^{Q_d} i\boldsymbol{\pi}_i$. The average packet arrival rate is equal to $k_d\eta_d$ according to (1). Thus, the average queuing delay is derived based on Little's Law [25] as

$$\boldsymbol{D}_{av} = \frac{1}{k_d\eta_d}\sum_{i=1}^{Q_d} i\boldsymbol{\pi}_i \tag{13}$$

Next, we discuss the analytical expressions of the average power consumption. Notice that only when no harvested energy but data packets waiting for transmission, the reliable energy source will be possibly used if the transmission channel is available. Thus, the power consumption from grid-powered only depends on two probabilities $\lambda_{1,i}$ and $\mu_{1,i}$.

Theorem 2. *The average power consumption $\boldsymbol{P}_{av}$ drawn from the reliable energy source is obtained as*

$$\boldsymbol{P}_{av} = \sum_{i=0}^{Q_d}\xi_i\pi_{(i,0)} - \sum_{i=0}^{Q_d}\zeta_i\pi_{(i,1)}, \tag{14}$$

where

$$\begin{aligned}\xi_0 &= (\rho_0 + \bar{\alpha}_3)Q_d + \rho_2\\ \xi_i &= \eta_e\bar{\alpha}(Q_d - i) + \rho_2 - \alpha_0\\ \zeta_0 &= \alpha_2 Q_d\\ \zeta_i &= \bar{\eta}_e\alpha(Q_d - i) + \alpha_1\end{aligned} \tag{15}$$

for $i \in \{0, 1, \cdots, Q_d\}$.

Proof. As discussed above, the normalized average power consumption from grid-powered can be obtained as

$$\boldsymbol{P}_{av} = \sum_{i=0}^{Q_d}\pi_{(i,0)}\rho_2\alpha g_i - \sum_{i=1}^{Q_d}\pi_{(i,0)}\rho_1\alpha f_i \tag{16}$$

By inserting $\rho_2\alpha g_i = \rho_2 - \lambda'_{1,i-1}$ and $\rho_1\alpha f_i = \tilde{\mu}_{1,i} - \alpha_0$ into (16) and extracting $\boldsymbol{P}_{av}$, we arrive at

$$\boldsymbol{P}_{av} = \rho_2\sum_{i=0}^{Q_d}\pi_{(i,0)} - \alpha_0\sum_{i=1}^{Q_d}\pi_{(i,0)} + \sum_{i=1}^{Q_d}\left(\pi_{(i,0)}\tilde{\mu}_{1,i} - \pi_{(i-1,0)}\lambda'_{1,i-1}\right). \tag{17}$$

From the Markov chain shown in Figure 4, the local balance equation at state $(i,0)$ can be expressed as

$$\pi_{(i+1,0)}\tilde{\mu}_{1,i+1} - \pi_{(i,0)}\lambda'_{1,i} = \begin{cases}(\rho_0 + \bar{\alpha}_3)\pi_{(i,0)} - \alpha_2\pi_{(i,1)} - \alpha_1\pi_{(i+1,1)} & i = 0\\ (\tilde{\mu}_{1,i} + \eta_e\bar{\alpha})\pi_{(i,0)} - \alpha_2\pi_{(i,1)} & \\ -\pi_{(i-1,0)}\lambda'_{1,i-1} - \alpha_1\pi_{(i+1,1)} & i \geq 1\end{cases} \tag{18}$$

For the partition function, we rewrite the second section and obtain

$$\begin{aligned}\pi_{(i+1,0)}\tilde{\mu}_{1,i+1} - \pi_{(i,0)}\lambda'_{1,i} = {}&\left(\pi_{(i,0)}\tilde{\mu}_{1,i} - \pi_{(i-1,0)}\lambda'_{1,i-1}\right)\\ &+ \eta_e\bar{\alpha}\pi_{(i,0)} - \alpha_2\pi_{(i,1)} - \alpha_1\pi_{(i+1,1)}\end{aligned} \tag{19}$$

for all $i \geq 1$. Through recursion of (19) and by inserting $\pi_{(1,0)}\tilde{\mu}_{1,1} - \pi_{(0,0)}\lambda'_{1,0}$ given by (18), we can further get

$$\begin{aligned}\pi_{(i+1,0)}\tilde{\mu}_{1,i+1} - \pi_{(i,0)}\lambda'_{1,i} = {}&\eta_e\bar{\alpha}\sum_{m=1}^{i}\pi_{(m,0)} - \alpha_2\sum_{m=0}^{i}\pi_{(m,1)}\\ &- \alpha_1\sum_{m=1}^{i}\pi_{(m,1)} + (\rho_0 + \bar{\alpha}_3)\pi_{(0,0)}\end{aligned} \tag{20}$$

By substituting (20) into (17), we can express the average power $\boldsymbol{P}_{av}$ as

$$\begin{aligned}\boldsymbol{P}_{av} = {}&((\rho_0 + \bar{\alpha}_3)Q_d + \rho_2)\pi_{(0,0)} - \alpha_2 Q_d\pi_{(0,1)}\\ &+ \sum_{i=1}^{Q_d}(\eta_e\bar{\alpha}(Q_d - i) + \rho_2 - \alpha_0)\pi_{(i,0)}\\ &- \sum_{i=1}^{Q_d}(\bar{\eta}_e\alpha(Q_d - i) + \alpha_1)\pi_{(i,1)}\end{aligned} \tag{21}$$

which perfectly corresponds to the (14) and (15). □

Therefore, by eliminating the dependence of $\boldsymbol{P}_{av}$ on the parameters g_i and f_i, the $\boldsymbol{P}_{av}$ have converted into a linear function of the steady-state probabilities $\pi_{(i,j)}$. Since the analytical expressions of both average queuing delay and average power consumption are determined by steady-state probability, we can achieve the excepted scheduling strategy by optimizing $\{\pi_{(i,j)}\}$, which is debated in Section 4.

3.2. Delay Minimization Problem under Power Constrained. We can find that the average delay is a linear combination of the steady-state probabilities in (13), so it can be minimized by restricting the steady-state probabilities. In addition, the average power consumption is also a linear function of the steady-state probabilities and coefficients are related to the transition probabilities in (21). Furthermore, the relationship between power consumption limitation and delay optimization can be established through the steady-state probabilities. Meanwhile, some transition probabilities can be expressed by the transmission parameters g_i and f_i, so we can get several constraints.

Due to $g_i \in [0, 1]$ and $f_i \in [0, 1]$, the transition probabilities $\lambda'_{1,i} = \rho_2\alpha(1-g_i) + \rho_2\bar{\alpha}$ and $\tilde{\mu}_{1,i} = \rho_1\alpha f_i + \alpha_0$ should satisfy the following inequalities

$$\rho_2\bar{\alpha} \le \lambda'_{1,i} \le \rho_2 \tag{22}$$

$$\alpha_0 \le \tilde{\mu}_{1,i} \le \bar{\eta}_d\alpha \tag{23}$$

In (22), we get the minimum of $\lambda'_{1,i}$ called $\rho_2\bar{\alpha}$ when $g_i = 1$ and the maximum called ρ_2 when$g_i = 0$. However, we get the minimum of $\tilde{\mu}_{1,i}$ called α_0 when $f_i = 0$ and the maximum called $\bar{\eta}_d\alpha$ when $f_i = 1$ in (23). Consequently, recalling the local balance equation (12), we can obtain the following the steady-state probabilities constraint

$$\gamma\boldsymbol{\pi}_{i-1} \le \boldsymbol{\pi}_i \le \gamma\boldsymbol{\pi}_{i-1} + \bar{\eta}_e\pi_{(i,0)} + \delta\bar{\eta}_e\pi_{(i-1,0)} \tag{24}$$

where $\delta = \eta_d/\bar{\eta}_d$ and $\gamma = \bar{\alpha}\eta_d/\alpha\bar{\eta}_d$. Let $\boldsymbol{P}_{\max}$ denotes the upper bound of allowable power from reliable energy source. Based on the above constraints and the scheduling probability as the optimization variable, the average delay minimum problem under given power restriction is established as follows

$$\min_{\pi_{(i,j)}} \boldsymbol{D}_{av} = \frac{1}{k_d\eta_d}\sum_{i=1}^{Q_d} i\boldsymbol{\pi}_i \qquad (a)$$

$$s.t.\begin{cases} \sum_{i=0}^{Q_d}\xi_i\pi_{(i,0)} - \sum_{i=0}^{Q_d}\zeta_i\pi_{(i,1)} \le \boldsymbol{P}_{\max} & (b) \\ \gamma\boldsymbol{\pi}_{i-1} \le \boldsymbol{\pi}_i \le \gamma\boldsymbol{\pi}_{i-1} + \bar{\eta}_e\pi_{(i,0)} + \delta\bar{\eta}_e\pi_{(i-1,0)} & (c) \\ \pi_{(i,j)} \ge 0 & (d) \\ \sum_{i=0}^{Q_d}\sum_{j=0}^{Q_e}\pi_{(i,j)} = 1 & (e) \\ & (f) \\ \boldsymbol{\Lambda\pi} - \boldsymbol{\pi} = \boldsymbol{0} \end{cases} \tag{25}$$

In problem (25), the objective and the first constraint are exactly the average queuing delay and the paid power consumption. Constraint (25.c) represents the mapping from the scheduling probabilities to the steady-state probabilities. Constraints (25.d)- (25.f) indicate the properties of the Markov chain. Problem (25) is a linear programming (LP) problem with the steady-state probabilities being the variables. With the optimal solution$\pi^*_{(i,j)}$, we can obtain the optimal scheduling probabilities g_i^* and f_i^* as shown in the sequel.

4. Solution of Optimization Problem

In this subsection, we will discuss how to seek the optimal solution $\pi^*_{(i,j)}$ of the 2-D Markov chain to attempt solving the optimization problem (25), and how to further derive all optimal transmission parameters $\{g_i^*\}$ and $\{f_i^*\}$.

4.1. The Optimal Steady-State Probability. The (25) is a formulation of the LP problem with the stead-state probabilities being the variable. However, due to the complexity of 2-D state transitions, it is difficult to derive a closed-form optimal solution of the corresponding LP problem.

For the purpose of reducing latency, the scheduling policy should send data packets continually, which makes the queue of data packet not too large. On the other side, for the purpose of cutting down the average power consumption from the reliable energy source, the scheduling policy prefers to wait for the harvested energy when the energy queue is none, which leads to an increase in the length of data queue. As a result, there exists an optimal threshold imposed on the data queue length, $i^* \in \{0, 1, \cdots, Q_d\}$. When the data queue length exceeds the threshold, the source transmits using the reliable energy, otherwise it waits for the harvested energy. Therefore, the transmission could consume more energy from the reliable energy source with the threshold decreasing. It further shows that the optimal threshold is determined by the power constraint $\boldsymbol{P}_{\max}$ from the reliable energy source.

Given all of that, combining with (24), we can obtain the optimal solution $\pi^*_{(i,j)}$ corresponding to the threshold i^* and $\boldsymbol{P}_{\max}$ based data transmission scheme [9], as follows

$$\begin{gathered} ((\rho_0 + \bar{\alpha}_3)Q_d + \rho_2)\pi_{(0,0)} - \alpha_2 Q_d\pi_{(0,1)} = \boldsymbol{P}_{\max}, \\ \gamma\sum_{j=0}^{Q_e}\pi^*_{(i-1,j)} - \sum_{j=0}^{Q_e}\pi^*_{(i,j)} = 0, \ (1 \le i \le i^* - 1), \\ \gamma\sum_{j=0}^{Q_e}\pi^*_{(i-1,j)} + \bar{\eta}_e\left(\pi^*_{(i,0)} + \delta\pi^*_{(i-1,0)}\right) - \sum_{j=0}^{Q_e}\pi^*_{(i,j)} = 0, \ (i^* + 1 \le i \le Q_d). \end{gathered} \tag{26}$$

In order to derive all $\{\pi^*_{(i,j)}, 0 \le i \le Q_d, 0 \le j \le Q_e\}$ from (26), a multidimensional matrix calculation is constructed by adding two constraints (25.e) and (25.f)

$$\boldsymbol{\Gamma}_{N\times N} \cdot \boldsymbol{\pi}^*_{N\times 1} = [\boldsymbol{P}_{\max}, 0, \cdots, 1]^T_{1\times N}, \tag{27}$$

where $\boldsymbol{\Gamma}$ is a $N \times N$ coefficient matrix, and $N = (1 + Q_d)(1 + Q_e)$. Through (27), we can calculate all optimal steady-state probabilities $\{\pi^*_{(i,j)}\}$ by solving N independent linear equations.

4.2. The Optimal Transmission Parameters. For ease of discussion, we suppose $\boldsymbol{P}_{con}$ is the power consumption when the RSU always use the reliable power for transmitting. Due to the limit of $\boldsymbol{P}_{\max}$, there are two different situations [9], as following.

Situation 1: $\boldsymbol{P}_{con} \le \boldsymbol{P}_{\max}$, which means there are enough reliable power can be used for transmitting when it needs. In this case, the optimal threshold satisfies $i^* = 0$. It presents that the RSU delivers one packet if the data buffer is nonempty and the transmission channel is "*on*," without concern for whether the harvested energy queue is empty. Furthermore, the optimal transmission parameters are given by $g_i^* = 1(i^* \ge 0)$ and $f_i^* = 1(i^* > 0)$.

Situation 2: $\boldsymbol{P}_{con} > \boldsymbol{P}_{\max}$, which means the reliable power is limit. Then, it is necessary to balance the use of energy from the reliable energy source to achieve the optimal problem (25). In this case, the utilization of power from the reliable energy source could happen only in the case $\boldsymbol{q}[n-1] = (i, 0)$ when new data packets arrive and the transmission channel is available but the harvested energy queue is empty. According to the above threshold strategy, if $(q_d[n-1] + d[n]) > i^*$ and $\boldsymbol{s}[n] = (\cdot, \cdot, 'on')$, the source should transmit data packet with probability "1" even though no harvested energy. So, the optimal transmission parameters g_i^* and f_i^* are set to 1. In contrast, if $(q_d[n-1] + d[n]) < i^*$, the source need to silently wait for the harvested energy whether new data arrives or not. Here, g_i^* andf_i^* are set to 0. But, when $(q_d[n-1] + d[n]) = i^*$, the source transmits using the reliable power with $g_i^* < 1$ and $f_i^* < 1$ in order to obtain the minimum average delay $\boldsymbol{D}_{av}^*$ under the power constraint $\boldsymbol{P}_{\max}$.

In order to obtain g_i^* and f_i^* at the optimal threshold, we recall the local balance equation with the optimal steady-state probabilities $\pi_{(i,j)}^*$ at state (i, j), and have

$$\bar{\eta}_d \alpha \boldsymbol{\pi}_{i^*}^* - \eta_d \bar{\alpha} \boldsymbol{\pi}_{i^*-1}^* = \left(\lambda_{1,i^*-1}' - \bar{\alpha}_2\right)\pi_{(i^*-1,0)}^* + \left(\bar{\eta}_d \alpha - \tilde{\mu}_{1,i^*}\right)\pi_{(i^*,0)}^* \tag{28}$$

By substituting $\lambda_{1,i^*-1}' = \rho_2(1 - \alpha g_{i^*-1}^*)$ and $\tilde{\mu}_{1,i^*} = \rho_1 \alpha f_{i^*}^* + \alpha_0$ into (28), we can get

$$\rho_2(1 - \alpha g_{i^*-1}^*)\pi_{(i^*-1,0)}^* = \bar{\eta}_d \alpha \boldsymbol{\pi}_{i^*}^* - \eta_d \bar{\alpha} \boldsymbol{\pi}_{i^*-1}^* - \alpha_1(1 - f_{i^*}^*)\pi_{(i^*,0)}^* + \bar{\alpha}_2 \pi_{(i^*-1,0)}^* \tag{29}$$

In (29), $f_{i^*}^*$ denotes the optimal transmission probability when $\boldsymbol{q}[n-1] = (i^*, 0)$ and $\boldsymbol{s}[n] = (\cdot, \cdot, 'on')$. Although the data queue length has reached the threshold and no harvested energy is available at the end of last timeslot, no new data packet arrives at the n-th timeslot. For the convenience, $f_{i^*}^* = 0$ is acceptable and reasonable. So that, we can get all transmission parameters as follow

$$g_i^* = \begin{cases} 0 & i < i^* - 1 \\ 1 - \dfrac{\bar{\eta}_d \alpha \boldsymbol{\pi}_i^* - \eta_d \bar{\alpha} \boldsymbol{\pi}_{i-1}^* - \alpha_1 \pi_{(i,0)}^*}{\alpha_2 \pi_{(i-1,0)}^*} & i = i^* - 1 \\ 1 & i > i^* - 1 \end{cases} \tag{30}$$

$$f_i^* = \begin{cases} 0 & i \le i^* \\ 1 & i > i^* \end{cases} \tag{31}$$

From (30) and (31), the transmit probabilities are only determined by the comparison between the data queue length and the threshold value. Due to the limit of reliable power consumption, RSU waits for the harvested energy when the data queue length is less than or equal to the threshold, but when the data queue length exceeds the threshold, one packet is sent by the reliable power over downlink wireless channel. Therefore, the optimal scheduling policy can be described as a threshold-based policy.

5. Simulation Results

In simulations, the data packet and energy packet arrival processes in the RSU are modelled by generating two Bernoulli random variables with the parameters η_d and η_e at the beginning of each time slot, respectively. The number of newly arrived data and energy packets is separately less than 2 in each time slot. We adopt two-state "*on*/*off*" channel model to describe the RSU-to-vehicle downlink communication link state. The packet transmission is scheduled according to the optimal transmission parameters $\{g_i^*\}$ and $\{f_i^*\}$ in (30) and (31). Each simulation runs over 10^6 time slots.

We simulate and discuss the optimal queuing delay and reliable power consumption trade-off performance in terms of battery capacity, packet arrival rate and channel availability rate. The results are shown in Figures 5–7. Figure 5 plots the trade-off under different queue length of harvested energy Q_e, where the data packet and energy arrival rates in RSU are same, as $\eta_d = \eta_e = 0.3$. In Figure 5, the theoretical results are presented as the lines, while the simulation results are marked by symbol "∘." In addition, we use the Linprog optimization tool to solve the LP problem (25) in order to further verify the correctness of the theoretical solution, and use the maker "+" to demonstrate the Linprog results. We can see that theoretical results are in good agreement with the simulation and Linprog results from Figure 5. It is observed that the average minimum queuing delay decreases when the average power increases, and when the available power decreases and approaches a critical value, the queuing delay will increase dramatically and grow to infinity. Besides, the decreasing rate grows with the increase of the battery capacity Q_e. This means that a larger Q_e leads to a much smaller queuing delay, since less harvested energy is wasted due to the limitation of the battery capacity. For the sake of brevity, the Linprog results will be omitted in the following simulation diagrams.

Figure 6 focuses on the impact of different energy arrival rates η_e on the trade-off curve, where the data packet arrival rates is set to $\eta_d = 0.3$. From Figure 6, we show that the comparison between the energy arrival rate and the data package arrival rate has a great influence on the whole delay-power trade-off curve. Given the identical queue length and data packet arrival rate, a greater average power will be induced for lower harvested energy arrival rate, besides that the

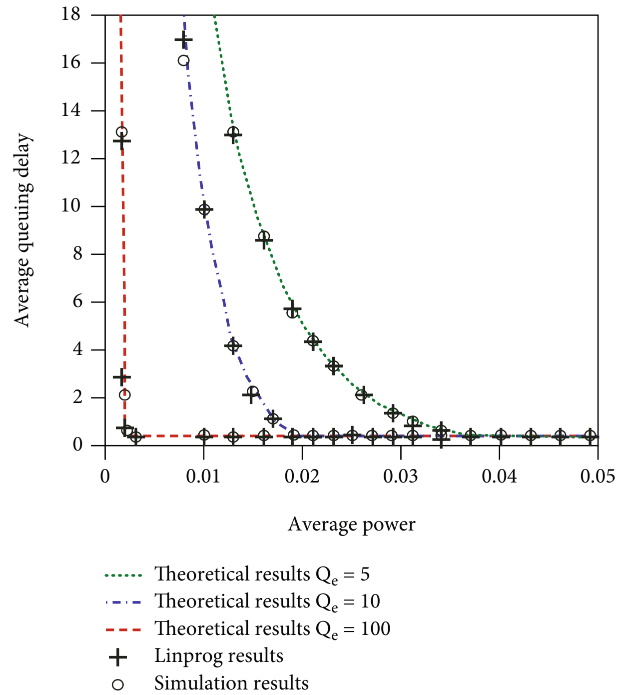

FIGURE 5: The optimal delay-power curves for different Q_e. ($\eta_d = \eta_e = 0.3$, $Q_d = 45$).

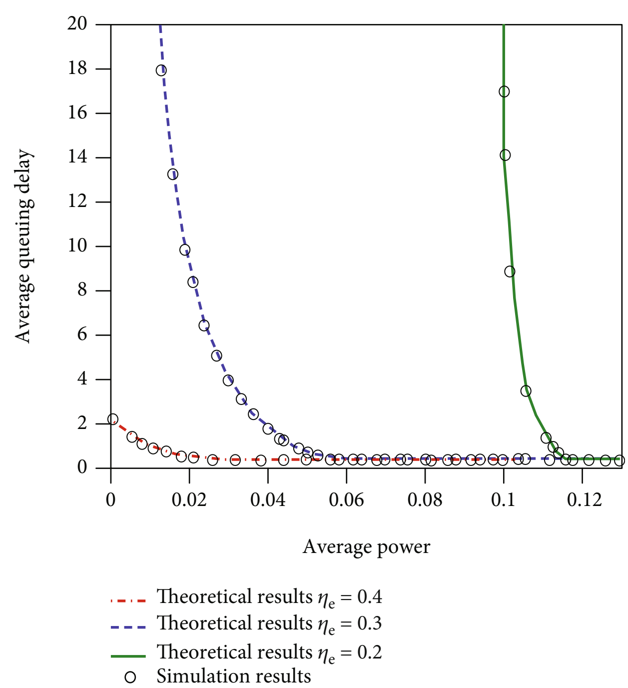

FIGURE 6: The optimal delay-power curves for different energy harvesting rate η_e ($\eta_d = 0.3$, $Q_d = 45$, $Q_e = 5$).

delay-power curves change steeper. It is because that the RSU must exploit more extra reliable energy source power to transmit backlogged packets waiting when the energy arrival rate is less than the data package arrival rate $\eta_e < \eta_d$. Conversely, the RSU has enough harvested energy to transmit data packets when $\eta_e > \eta_d$. Moreover, there has the less average delay even if $\boldsymbol{P}_{\max} = 0$.

Figure 7 shows the optimal queuing delay and reliable power consumption trade-off under different probabilities of RSU-to-vehicle downlink availability rate, α =0.5, 0.6, 0.8 and 1. The average queuing delay decreases with the average power increasing, as expected. For each numerical curve, when the reliable power become large enough which means there always exists energy for transmitting if needed,

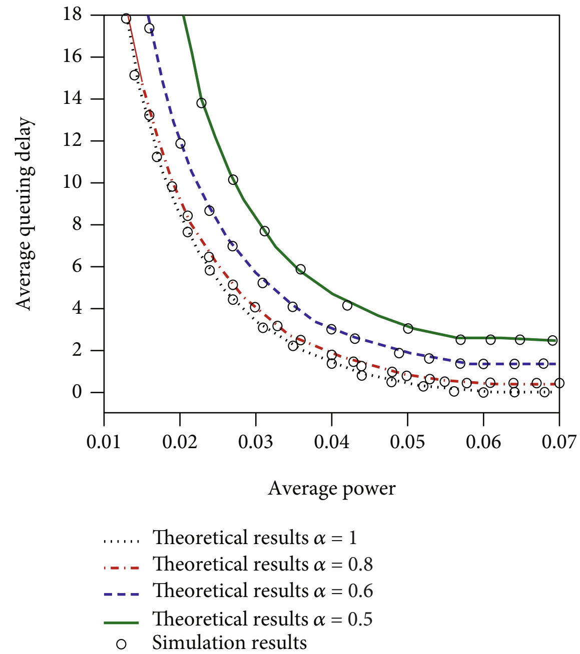

FIGURE 7: The delay-power curve for different α. ($\eta_d = \eta_e = 0.3$).

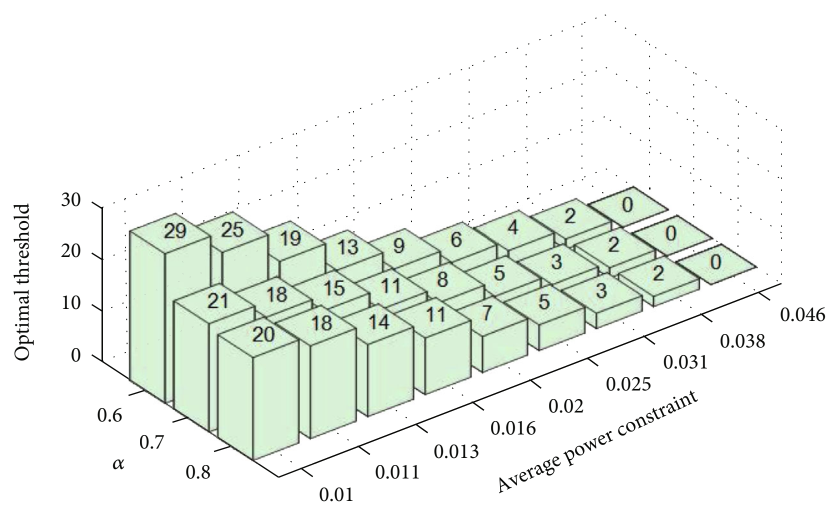

FIGURE 8: The threshold structure of optimal scheduling policy.

the average queuing delay of RSU only depends on the data packets arrival and the available rate of the channel and remains same. Meanwhile, we can see that, the smaller the availability rate of the channel is, the greater the average queuing delay is. This is because more timeslots will stay in the "*on*" state and can be used for transmitting.

Next, we verify that the optimal scheduling policy is determined by the data queue threshold i^* and the transmission parameters $\{g_i^*\}$ and $\{f_i^*\}$. Figure 8 shows the optimal threshold i^* value responding to the assigned average reliable power constraint $\boldsymbol{P}_{\max}$ when the availability rate of downlink channel α=0.6, 0.7 and 0.8, respectively. The threshold-power curve shows ladder-type decline in whichever given α. With the increasing of the disposable power constraint, the optimal threshold decreases slowly since the RSU could afford to transmit more frequently without harvested energy when the channel is "*on*" state. Furthermore, as the channel availability rate increases, the optimal threshold i^* decreases gradually under the same reliable power limit because the RSU has more opportunities to send queuing data to passing vehicle within the coverage of RSU.

In Figure 9, we demonstrate the theoretical results to confirm the threshold-based structure of the optimal scheduling policy expressed by (30) and (31), where $\eta_e = \eta_d = 0.4$ and $\alpha = 0.7$. What is more, the transmission parameters bring to light a threshold-based structure imposed on the data queue length under reliable power constraints. From Figure 9(a), we can find that the optimal threshold is queue length "8," and transmission parameters are set as $g_7^* = 0.597$, $g_i^* = f_i^* = 1 (i \geq 8)$, which is the idea of threshold-

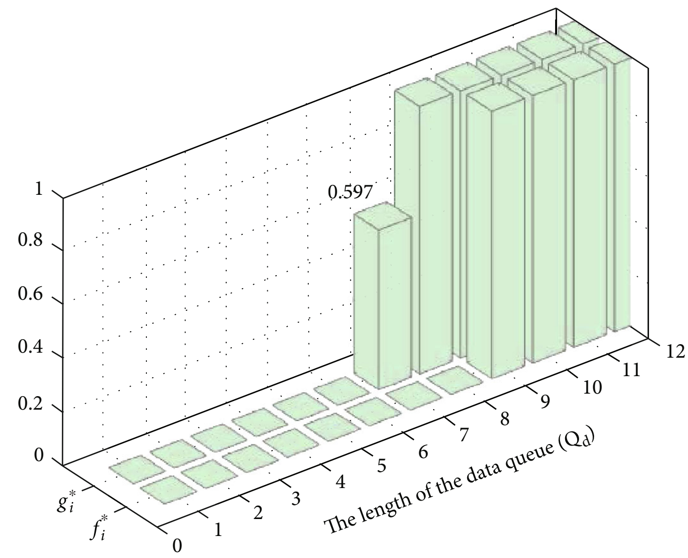

(a)

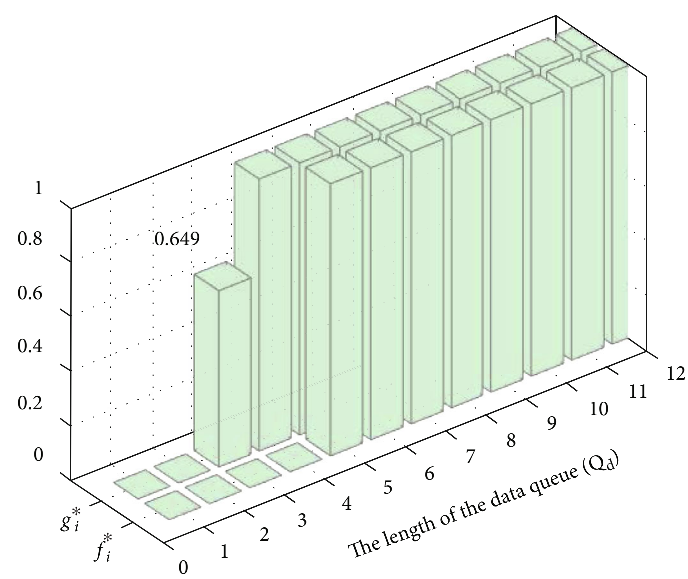

(b)

Figure 9: The threshold-based scheduling policy. (a) $\boldsymbol{P}_{\max} = 0.02$, ($b$) $\boldsymbol{P}_{\max} = 0.03$.

based policy. However, it is queue length "4" and $g_3^* = 0.649$, $g_i^* = f_i^* = 1 (i \geq 4)$in Figure 9(b). Though it is relatively easier to dispatch data packets when the communication channel is usable in Figure 9(b), it leads to a higher reliable power consumption in RSU at cost. In other words, the RSU makes good use of the power resource from reliable energy source by regulating the optimal threshold point for different power constraints.

6. Conclusions

In this paper, we investigated the delay-minimal scheduling problem with the supply of hybrid energy sources for RSU-to-vehicle downlink communication in CVIS. The RSU is powered by a limited capacity energy harvesting battery, coupled with a reliable energy constrained by maximum power consumption. By establishing probabilistic scheduling policy and modelling the two-dimensional Markov chain, we formulated the expressions of delay and reliable power consumption, and construct an optimization LP problem with the steady-state probability as variables. For solving the steady-state probability problem caused by the complexity of local equations, the analytical solution of the optimal transmission parameters can be obtained by threshold piecewise optimization. It has been proved that the optimal scheduling policy is threshold-based, that is, the use of reliable power resource for transmission should only occur when the data queue length exceeds optimal threshold while no harvested energy can be resorted if wireless channel is available. The optimal threshold is jointly decided by packet arrivals, downlink availability rate as well as the maximum reliable power constraint. At the end, simulation results confirmed our theoretical analysis. It was shown that there always exists an optimal delay and reliable power limit trade-off in RSU and its decreasing rate depends on the harvested energy arrival rate and the battery capacity. Moreover, the downlink availability rate increases, the optimal threshold decreases gradually under the same power consumption limit.

Data Availability

The data used to support the findings of this study are available from the corresponding author upon request.

Conflicts of Interest

The authors declare that there is no conflict of interest regarding the publication of this paper.

Acknowledgments

The authors would like to thank the supports of Scientific and Technological Key Project of “Revealing the List and Taking Command” in Heilongjiang Province (2021ZXJ02A02), the National Natural Science Foundation (61102105), and the Harbin Artificial Intelligence Association Key Project (ZKYLX004).

References

[1] Y. Lv, Y. Duan, W. Kang, Z. Li, and F.-Y. Wang, “Traffic flow prediction with big data: a deep learning approach,” *IEEE Transactions on Intelligent Transportation Systems*, vol. 16, no. 2, pp. 865–873, 2015.

[2] X. Fan, C. Huang, J. Zhu, and B. Fu, “Replication-Based Data Dissemination in Connected Internet of Vehicles,” *Wireless Communications and Mobile Computing*, vol. 2019, Article ID 2150524, 16 pages, 2019.

[3] L. Huang, H. Jiang, Z. Zhang, Z. Yan, and H. Guo, “Efficient data traffic forwarding for infrastructure-to-infrastructure communications in VANETs,” *IEEE Transactions on Intelligent Transportation Systems*, vol. 19, no. 3, pp. 839–853, 2018.

[4] C. Wang, J. Li, Y. He, K. Xiao, and H. Zhang, “Destination prediction-based scheduling algorithms for message delivery in iovs,” *IEEE Access*, vol. 8, pp. 14965–14976, 2020.

[5] M. M. Najm, M. Patra, and T. Venkatesh, “Cost-and-Delay aware dynamic resource allocation in federated vehicular clouds,” *IEEE Transactions on Vehicular Technology*, vol. 70, no. 6, pp. 6159–6171, 2021.

[6] J. Li, C. Wang, D. Seo et al., “Deep Learning-Based Service Scheduling Mechanism for GreenRSUs in the IoVs,” *Wireless Communications and Mobile Computing (WCMC)*, vol. 2021, article 7018486, pp. 1–15, 2021.

[7] K. Tutuncuoglu and A. Yener, “Optimum transmission policies for battery limited energy harvesting nodes,” *IEEE Transactions on Wireless Communications*, vol. 11, no. 3, pp. 1180–1189, 2012.

[8] M. Patra and C. S. R. Murthy, “Performance evaluation of joint placement and sleep scheduling of grid-connected solar powered road side units in vehicular networks,” *IEEE Transactions on Green Communications and Networking*, vol. 2, no. 4, pp. 1197–1209, 2018.

[9] J. Liu, H. Dai, and W. Chen, “Delay optimal scheduling for energy harvesting based communications,” *IEEE Journal on Selected Areas in Communications*, vol. 33, no. 3, pp. 452–466, 2015.

[10] B. Ko, K. Liu, S. H. Son, and K. -J. Park, “RSU-assisted adaptive scheduling for vehicle-to-vehicle data sharing in bidirectional road scenarios,” *IEEE Transactions on Intelligent Transportation Systems*, vol. 22, no. 2, pp. 977–989, 2021.

[11] K. Liu, J. K. Ng, V. C. Lee, S. H. Son, and I. Stojmenovic, “Cooperative Data Scheduling in Hybrid Vehicular Ad Hoc Networks: VANET as a Software Defined Network,” *IEEE/ACM Transactions on Networking*, vol. 24, no. 3, pp. 1759–1773, 2016.

[12] Q. Ibrahim, “Design, implementation and optimisation of an energy harvesting system for vehicular ad hoc networks’ road side units,” *IET Intelligent Transport Systems*, vol. 8, no. 3, pp. 298–307, 2014.

[13] R. Atallah, M. Khabbaz, and C. Assi, “Energy harvesting in vehicular networks: a contemporary survey,” *IEEE Wireless Communications*, vol. 23, no. 2, pp. 70–77, 2016.

[14] A. A. Hammad, G. H. Badawy, T. D. Todd, A. A. Sayegh, and D. Zhao, “Traffic scheduling for energy sustainable vehicular infrastructure,” in *IEEE GLOBECOM*, pp. 1–6, Miami, FL, USA, 2010.

[15] W. S. Atoui, W. Ajib, and M. Boukadoum, “Offline and online scheduling algorithms for energy harvesting RSUs in VANETs,” *IEEE Transactions on Vehicular Technology*, vol. 67, no. 7, pp. 6370–6382, 2018.

[16] R. F. Atallah, C. M. Assi, and J. Y. Yu, “A reinforcement learning technique for optimizing downlink scheduling in an energy-limited vehicular network,” *IEEE Transactions on Vehicular Technology*, vol. 66, no. 6, pp. 4592–4601, 2017.

[17] L. Dai, T. Chen, Y. Zhai, and G. Wang, “Energy-Efficient Distributed Packet Scheduling Optimization Strategy in Cooperative Vehicle Infrastructure Systems,” *Wireless Communications and Mobile Computing (WCMC)*, vol. 2021, article 6661623, pp. 1–11, 2021.

[18] L. Dai, Y. Zhai, and G. Wang, “Packet scheduling scheme for energy-delay tradeoff in self-powered roadside units,” *Journal of Traffic and Transportation Engineering*, vol. 20, no. 2, pp. 161–171, 2020.

[19] A. Muhtar, B. Qazi, S. Bhattacharya, and J. Elmirghani, “Greening vehicular networks with standalone wind powered RSUs: a performance case study,” in *Proceedings of the IEEE International Conference on Communications*, pp. 4437–4442, Budapest, Hungary, 2013.

[20] B. Collins and R. L. Cruz, “Transmission policies for time varying channels with average delay constraints,” in *Proceedings of the Annual Allerton Conference on Communication Control and Computing*, pp. 709–717, Monticello, IL, 1999.

[21] S. Zhang, A. Hafid, Z. Wang, H. Zhao, and S. Wang, “A cross-layer aware sensing-throughput tradeoff for Multi-Channel cognitive radio networks,” in *2015 IEEE 81st Vehicular Technology Conference (VTC Spring)*, pp. 1–5, Glasgow, UK, 2015.

[22] Q. Shi, L. Zhao, Y. Zhang, G. Zheng, F. R. Yu, and H. -H. Chen, “Energy-efficiency versus delay tradeoff in wireless networks virtualization,” *IEEE Transactions on Vehicular Technology*, vol. 67, no. 1, pp. 837–841, 2018.

[23] X. Liu, K. Hua, Z. Chen, A. S. Alghamdi, and M. N. Ali, “An Efficient Cross-layer Approach for Throughput-Maximal and Delay-Minimal Green Vehicular Networks,” in *2018*

International Conference on Computing, Networking and Communications (ICNC), pp. 652–658, Maui, HI, USA, 2018.

[24] J. Zhao, Y. Chen, and Y. Gong, "Study of connectivity probability of vehicle-to-vehicle and vehicle-to-infrastructure communication systems," in *2016 IEEE 83rd Vehicular Technology Conference (VTC Spring)*, pp. 1–4, Nanjing, China, 2016.

[25] L. Kleinrock, *Queueing Systems, Theory*, vol. 1, Wiley, Hoboken, NJ, USA, 1975.